International Journal for Multidisciplinary Research (IJFMR)
E-ISSN: 2582-2160 ● Website: www.ijfmr.com ● Email: editor@ijfmr.com

Synthesis of Lead Zirconium Titanate [$PbZr_{0.52}Ti_{0.48}O_3$] (PZT) nano Powder by Sole-gel and Study the Dielectric and Ferroelectric Properties

Mr. Hitesh D. Sonawane

Research Student, Physics, Research Centre In Physics, M.S. G. Arts, Science & Commerce College, Malegaon

Abstract:
Lead Zirconium Titanate [$PbZr_{0.52}Ti_{0.48}O_3$] (PZT) nanocrystalline powder was successfully prepared using the sol-gel synthesis route. The obtained material was characterized through XRD, FTIR, UV–Visible spectroscopy, and SEM analysis. The XRD and FTIR results confirm the formation of a pure perovskite PZT phase without any detectable pyrochlore impurities after calcination at 700 °C. XRD analysis further indicates that the material crystallizes in a tetragonal structure with an approximate crystallite size of 26.5 nm. FTIR spectra display characteristic metal–oxygen vibration bands in the 400–800 cm^{-1} region, attributed to B–O bonding. The UV–Vis analysis shows an optical band gap close to 3 eV. SEM micrographs reveal that the particles exhibit a spherical morphology with noticeable agglomeration. Dielectric studies show that the PZT sample possesses a high dielectric constant, measured as $k \approx 817$ at 100 Hz and decreasing to about $k \approx 740$ at higher frequencies, while the dielectric loss remains low ($D \approx 0.02$). Ferroelectric (P–E) hysteresis investigation for the pellet sintered at 700 °C shows a remanent polarization (Pr) of approximately 2.7 μC/cm², a saturation polarization (Ps) near 8 kV/cm, and a coercive field (Ec) of around 5.1 kV/cm.

Keywords: PZT; Dielectric Measurement; Material Science; Sol gel; Energy Storage

1. Introduction:

Now a days, Nano-sized particles offer several advantages across various fields, including materials science, medicine, and electronics. Nanoscale materials improve the performance of electronic components, enabling faster and smaller devices. The unique properties of The Lead Zirconium Titanate [$PbZr_{0.52}Ti_{0.48}O_3$] (PZT) ceramics make them suitable for applications in sensors and actuators, with grain sizes less than 100 nm being particularly desirable for enhanced performance. Sol-gel method suitable for preparation of PZT nano particles powder.

This method allows for low calcining temperatures (as low as 600°C) and yields pure perovskite phase powders, which enhances the ferroelectric properties. The addition of citrate during the sol-gel process significantly influences the grain size and properties of the resulting ceramics, enabling better control over the final product's characteristics. Utilizing nanopowders can reduce the sintering temperature needed for PZT ceramics by approximately 100°C compared to conventional methods, while also enhancing their ferroelectric properties. PZT remains a pivotal material in electronics and mechanical engineering, with ongoing research focused on improving synthesis methods and expanding its applications. The advancements in low-temperature processing and film deposition techniques are particularly noteworthy for future developments. Lead Zirconium Titanate (PZT) is a good ferroelectric material and it is widely operated in memory devices, sensors actuators and energy storage devices [1,2]. The energy storage properties depend on crystalline size of synthesized PZT powder and such nano powder essential for making nao scale electronic devices [3]. PZT nano powder is used for the filler in polymer matrix to enhance dielectric properties and its applicable for as bypass capacitor, power capacitor and energy storage devices [1-3].PZT is solid solution having large piezo and pyroelectric coefficient. PZT exhibits a wide range of piezoelectric coefficients, typically from 200 to over 2000 pC/N, depending on the form and composition, with thin films and single crystals generally offering superior performance compared to ceramics. PZT (lead zirconate titanate) is recognized for its high piezoelectric coefficients, particularly due to the presence of a morphotropic phase boundary (MPB) where tetragonal and rhombohedral phases coexist. PZT materials near the MPB, such as PbZr0.52Ti0.48O3, have shown high piezoelectric coefficients due to their dual-phase structures, which enable enhanced electromechanical coupling. Specifically, studies highlight that ceramics synthesized at the MPB can achieve impressive outputs in piezoelectric applications. Research indicates that the coexistence of tetragonal and rhombohedral phases at the MPB leads to superior piezoelectric properties, as observed in the PMN-PZT system, where high piezoelectric coefficients were reported alongside reduced energy losses. There are two primary approaches to synthesize PZT (lead zirconate titanate) nanoparticles: the **top-down approach** and the **bottom-up approach**. In the top-down approach, there are different methods to synthesis of nano particles such **as**

1. **Mechanochemical Methods:** This method includes techniques like milling and attrition, which break down bulk materials into nanosized particles. For instance, studies have shown that the milling coprecipitation method effectively produces PZT nanopowders, resulting in significant enhancements in dielectric properties (Kim et al., 2004).
2. **Sol-Gel Process:** This widely used technique involves creating a colloidal solution that transforms into a gel, facilitating the formation of PZT nanoparticles. It has been noted that sol-gel synthesis can yield PZT nanoparticles with good quality and uniform morphology, suitable for large-scale production (Zak, 2012).
3. **Laser Ablation:** This method involves using laser energy to vaporize materials and form nanoparticles. Research indicates that laser ablation is an effective top-down approach, particularly for generating nanoparticles with controlled size and shape (Jiang et al., 2022).

Bottom-Up Approach

The synthesis of PZT nanoparticles can be achieved through several bottom-up fabrication routes, each offering specific benefits in terms of control, structure, and environmental impact. The sol–gel technique, although often associated with top-down processing, is widely recognized as a bottom-up pathway when nanoparticles are formed directly from atomic or molecular precursors. This approach provides excellent regulation over chemical composition and crystallinity, enabling the formation of uniform PZT particles with desirable structural properties (Miclea, 2012). Another widely used strategy is chemical precipitation, where suitable precursor solutions react to generate PZT nanoparticles. By modifying parameters such as reaction temperature, pH, and concentration, both particle size and morphology can be tailored effectively, making this method a flexible and adaptable bottom-up route (Khan et al., 2023). In addition, biogenic synthesis methods have recently gained attention. These approaches rely on biological materials—such as plant extracts, microorganisms, or enzymes—to facilitate nanoparticle formation. As a green chemistry technique, it reduces the need for hazardous reagents and supports environmentally conscious fabrication (Tripathy et al., 2023). Overall, the sol–gel method stands out as one of the most effective techniques, as it offers strong control over elemental composition, supports lower processing temperatures, promotes uniform particle distribution, and aligns well with sustainable processing requirements.

This study introduces several innovative contributions to the field of dielectric materials, including the synthesis of nanocrystalline $PbZr_{0.52}Ti_{0.48}O_3$ (PZT) particles through a sol-gel method. The process produces a perovskite crystal structure at a temperature of 700°C. A comprehensive examination of the PZT nanoparticles was carried out using techniques such as X-Ray diffraction, Fourier transform spectroscopy (FTIR), UV-Vis spectroscopy, and SEM, providing in-depth insights into their structural, morphological, and electronic characteristics. The results highlight the significance of PZT in advancing high-performance dielectric and ferroelectric materials, which are essential for next-generation electronic devices.

2. Experimental Procedure:

2.1 Materials

Starting materials to prepare the precursor solutions for PZT –nano particles was given by:

Lead acetate trihydrate ($Pb(CH_3COO)_2.3H_2O$, Merk), Titanium isopropoxide ($Ti(OCH(CH_3)_2)_4$, Merk), Zirconium n-propoxide ($Zr(OCH_2CH_2CH_3)_4$,70% in L-propanol, sigma-Aldrich), and 2-methoxyethanol ($CH_3OC_2H_4OH$, merk)

2.2 Synthesis:

To begin the synthesis, 11.65 g of lead acetate was dissolved in 50 mL of 2-methoxyethanol and magnetically stirred for 1 hour at room temperature. In a separate step, 7.2 mL of zirconium n-propoxide was mixed with 80 mL of 2-methoxyethanol and stirred for 30 minutes under the same conditions. After achieving a uniform mixture, 4.4 mL of titanium isopropoxide was introduced into the zirconium precursor solution, and an additional amount of solvent was added to adjust the total volume to 100 mL. This mixture was then stirred again for 30 minutes at room temperature to ensure homogeneity. During continuous stirring, the previously prepared lead solution was gradually poured into the zirconium–titanium mixture, and the combined solution was heated to 60 °C, maintaining stirring for another 30 minutes. The pH was carefully adjusted to 5 by adding a controlled quantity of distilled water. Within a few minutes, the transparent solution turned milky white, indicating the onset of gel formation. The obtained gel was subjected to drying, followed by grinding to obtain a fine powder. Finally, the dried material was calcined at 700 °C with a heating rate of 5 °C/min for 1 hour to eliminate organic residues completely. This heat treatment resulted in the formation of a yellow PZT nanopowder, confirming successful synthesis.

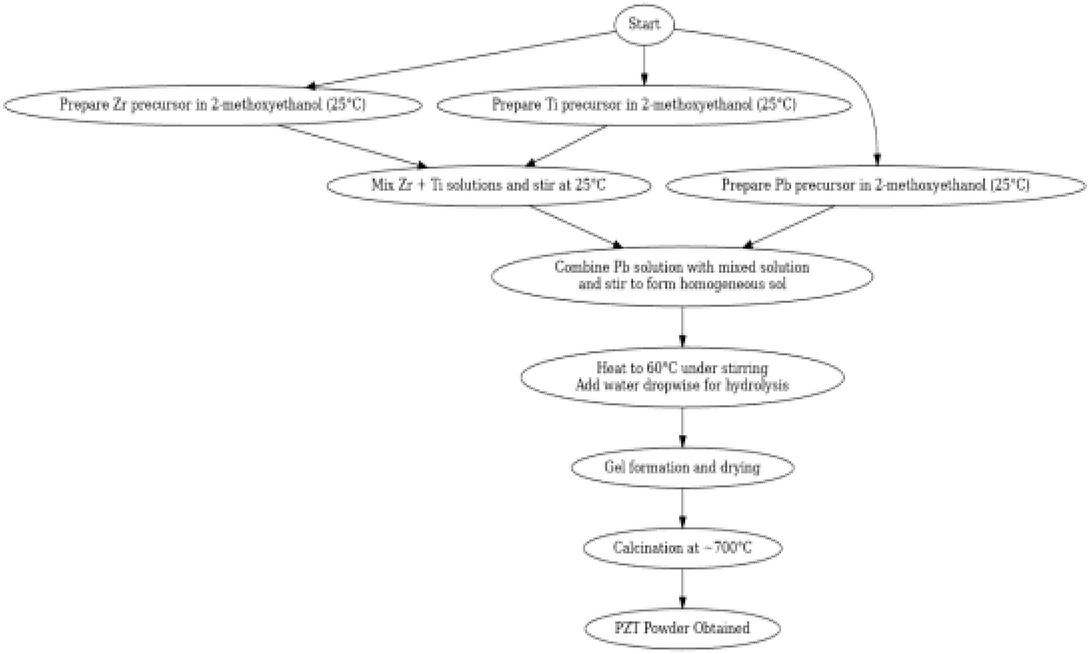

Fig. 1 flowchart of synthesis of PZT nano particles by sol-gel method

3. Characterization techniques:

X-ray diffraction analysis for the Lead Zirconium Titanate [$PbZr_{0.52}Ti_{0.48}O_3$] (PZT) powder was performed using a BRUKER D8 ADVANCE X-ray diffractometer. The FTIR spectra for PZT powder were obtained with a JASCO V-670 FTIR spectrometer operating in the 400–4000 cm^{-1} range. Optical characterization was carried out using a JASCO V-670 UV–Visible spectrophotometer, where the absorption spectra were recorded at room temperature over the 200–800 nm wavelength region. The microstructural features and surface morphology of PZT nano powder were examined using a Nova Nano SEM NPEP303 operated at 15 kV, which also provided elemental information. Dielectric properties were evaluated at room temperature within the 200 Hz to 6 MHz frequency window. An LCR bridge meter (NumetriQ-PSM1735) was employed to determine the dielectric parameters. The dielectric constant k was calculated from Equation (1):

$$k = \frac{C_p\, d}{\varepsilon_0 A} \qquad (1)$$

where $C_p$is the capacitance of the parallel plate sample, $d$represents the sample thickness, Adenotes the electrode contact area, and $\varepsilon_0 = 8.85 \times 10^{-12}$ F/cm is the permittivity of free space. Ferroelectric behaviors were assessed by analyzing variations in polarization under an applied electric field, which defines the ferroelectric response of the material. The polarization–electric field (P–E) hysteresis loop was measured using a modified Sawyer–Tower circuit (RT66A, Radiant Technologies, Walden, NY) at room temperature.

4 Results and Discussion: -

4.1 XRD analysis:

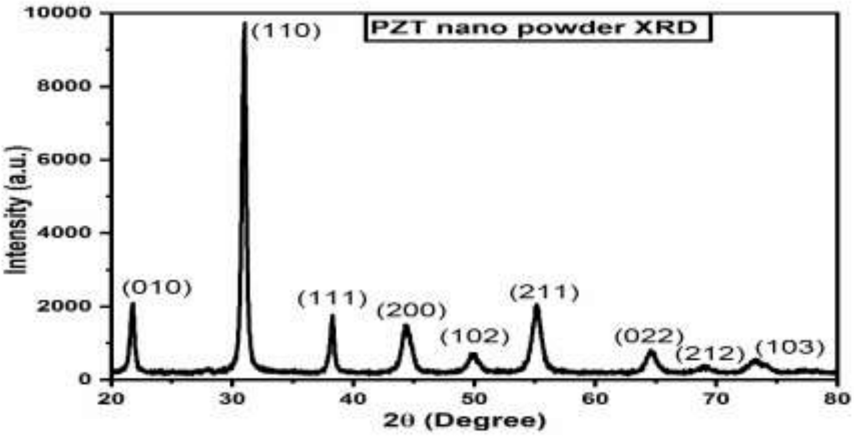

Fig. 2 X-Ray Diffraction pattern of $PbZr_{0.52}Ti_{0.48}O_3$ (PZT) nanoparticle

The X ray diffraction analysis of the synthesized PZT powder annealed at 700^0 C for 1 hour, is presented in figure 2. The diffraction pattern is measured using a Braker AXSD8 Advanced diffractometer, operating with CuKα radiation, and Scanned within the Braggs angle (2θ) range of 10^0 to 80^0. This instrumental configuration ensures high resolution peak identification and reliable structural characterization of powder sample. The XRD pattern, obtain the evidence of the formation of well-defined crystalline phase. The obtained diffraction peaks correspond to the perovskite structure of Lead Zirconate titanate (PZT), demonstrating the presence of a tetragonal crystal phase. The analysis of peak positions and intensities shows the close agreement with standard data, particularly when compared to the JCPDF/ICDD reference card no. 33-0784, which is commonly used for identification of tetragonal PZT. The matching peaks confirms the dominance of the desired perovskite phase and indicate the absence of major impurity phases such as pyrochlore. The lattice planes associated with the tetragonal perovskite structure can be indexed to the diffraction peaks observed at various 2θ values. The prominent reflections corresponding to the crystallographic planes (001), (110), (111), (200), (102), (211), (022), (212) and (103), each representing characteristic orientation of the tetragonal unit cell. This data validates the structural integrity of the synthesized PZT powder and confirm the successful phase formation.

Furthermore, the crystalline size of annealed PZT nano powder was estimated using Scherrer formula is given by

$$D = \frac{0.94*\lambda}{\beta cos\theta} \qquad (2)$$

Where, λ is the wavelength of the X-rays used (1.54 A^0), Θ is the angle, β is the FWHM of the peak (in radian). Scherrer formula which relates peak broadening to the dimensions based on the full width half maxima (FWHM) of major diffraction peak at 2θ= 21.74, the average crystalline size was calculated to be approximately 26.5nm. This nanoscale particle size implies that the PZT nano powder exhibits a high surface area and find grain structures which can significantly enhance the functional properties such as dielectric response and ferroelectric polarization activity.

2Θ (Degree)	**Crystalline Size (D) nm**	**Dislocation Density (δ) X 10^{-3} (nm^{-2})**	**Micro strain (ε) X 10^{-3}**

21.74	35.21	0.807	5.452
31.02	20.4	2.403	6.618
38.27	37.48	0.712	2.90
44.34	14.75	4.596	6.503
49.81	8.98	12.4	548.7
55.15	9.79	10.4	457.3
64.63	10.36	9.3	374.2

Table. 1 Crystalline Size, Dislocation Density and Macrostrain of PZT nano powder

Table 1 summarizes the key structural parameters of the PZT nanopowder obtained from XRD measurements at different diffraction angles (2θ). Crystallite sizes (D) were calculated using the Scherrer formula, while dislocation density (δ) and microstrain (ε) were evaluated through standard peak broadening analysis. The data show that the crystallite size varies between approximately 8.98 nm and 37.48 nm across the selected diffraction peaks. In general, smaller crystallite sizes are associated with higher dislocation densities and increased microstrain, indicating an inverse relationship between particle size and internal defects. This trend highlights the impact of nanoscale crystallinity on lattice distortion and the distribution of structural defects within the PZT material.

4.2 FTIR analysis:

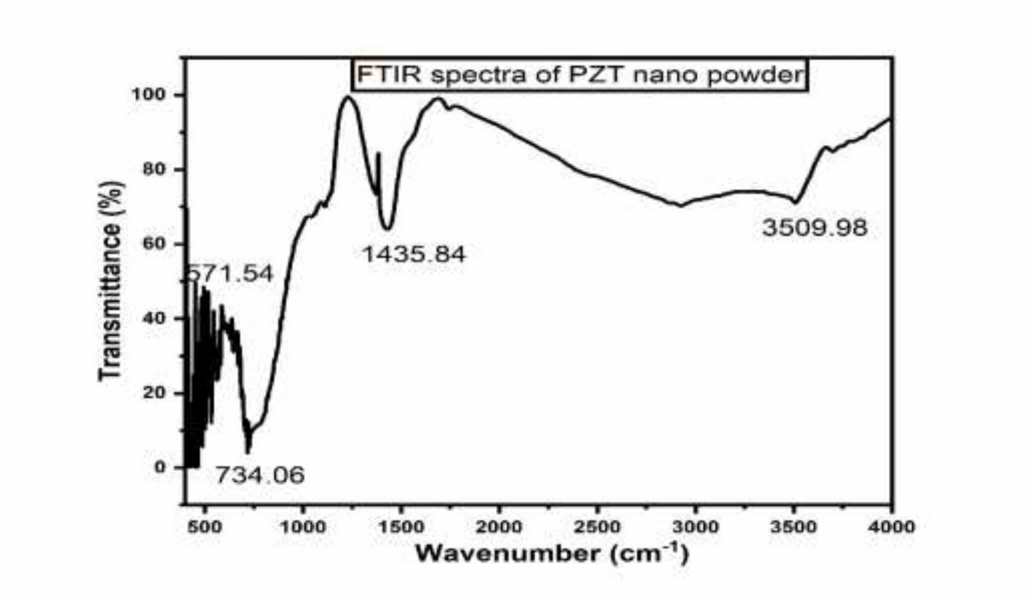

Fig. 3 FTIR spectrum of PZT

Fourier transform Infrared (FTIR) spectroscopy was utilized to examine the chemical and structural evolution of the precursor material during the heat treatment, which ultimately results in the formation of perovskite PZT. This analytical technique is particularly effective for identifying functional groups and monitoring the transformation of metal-oxygen networks as the material progresses from an amorphous or partially reacted state into a crystalline perovskite phase. The FTIR spectrum of PZT nano powder, recorded within the range 400-4000 cm^{-1} range corresponding to the sample calcined at 700^0C for 1hour, as illustrate in figure 3. In the obtained spectrum, several absorption peaks confirm the presence of fundamental vibrational modes associated with the spectrum units of the PZT lattice. The most notable features are located in low frequency region (approximately 280-750 cm^{-1}), where typical metal-oxygen stretching vibrations appear. Peaks detected near 560 cm^{-1} and 718 cm^{-1} are attributed to the Ti-O and Zr-O bonds vibrations, respectively. These peaks verify the formation of the BO_6 octahedral units, which represents a key structural element of the perovskite ABO_3 framework. Additionally, a broad absorption band around 3491 cm^{-1} is observed, which corresponds to O-H stretching vibrations. This indicates the presence of hydroxyl groups or adsorbed moisture, which is common in oxide materials, especially after thermal processing and cooling. The coexistence of metal-oxygen bands with minor O-H features confirm that the dominant phase is perovskite This result confirms the formation of perovskite structure of PZT calcined at 700^0C.

4.3 UV analysis:

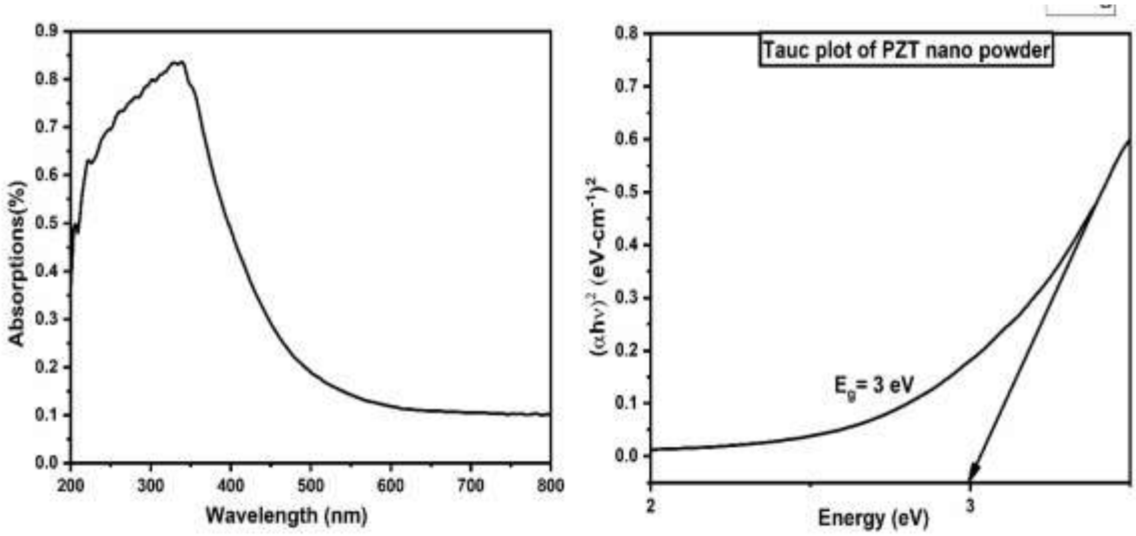

(a) **(b)**

Fig.-4 (a) UV-absorption spectra of PZT and (b) Graph of $(\alpha h\upsilon)^2$ versus photon energy (hν) for PZT powder

Figure 4(a) illustrate the absorption spectrum of the PZT nano powder as function of wavelength, while figure 4(b) represents the corresponding Tauc plot, where $(\alpha h\nu)^2$ is plotted against photon energy. In the absorption spectrum, a noticeable absorption peak is observed around 340nm, indicating a strong interaction between the incident photons and the material. This characteristics peak suggest that the material exhibits a significant optical response in the ultraviolet region, which is typically associated with electronic transitions from the valence band to conduction band. The Tauc plot illustrate in Figure 4(b) is used to determine the optical band gap of the PZT sample extending the linear region of the plot to the photon energy axis, the point of intersection provides the band gap value. This extrapolation method confirms that the PZT nano powder possesses a direct band gap. The calculated band gap energy approximately 3 eV, suggesting that the material suitable electronic and optical characteristics for applications in electronic devices and ferroelectric based components.

4.4 SEM Analysis:

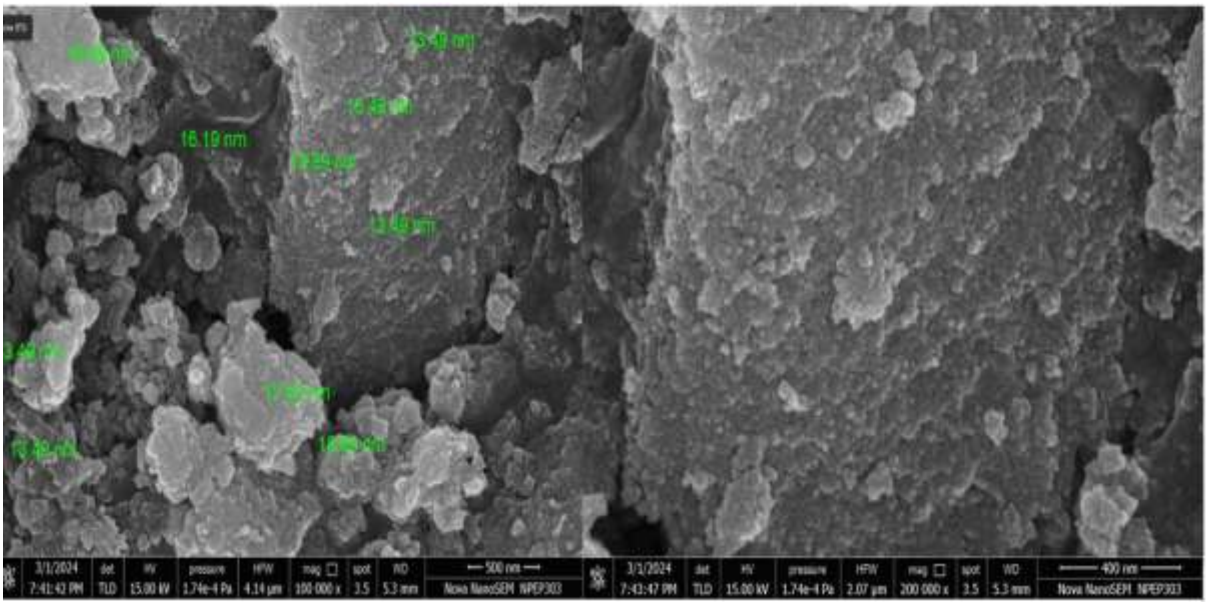

Fig. 5 SEM image of PZT nano particles

Figure 5 represents the SEM micrograph of the PZT nano powder calcined at 700^0C, revealing the presence of closely packed, fine particles with an average size of approximately 18nm. The particles exhibit a predominantly spherical morphology, and noticeable agglomeration is observed throughout the sample. This agglomeration likely occurs as a result of the elevated calcination temperature, which promotes sintering and enhances particle bonding. PZT smaller and uniform particles tends to form denser clusters due to influence of agglomeration. The SEM analysis confirms nanoscale particle formation and highlights the role of thermal treatment in driving the agglomeration behavior of the PZT powder.

4.5 Dielectric properties:

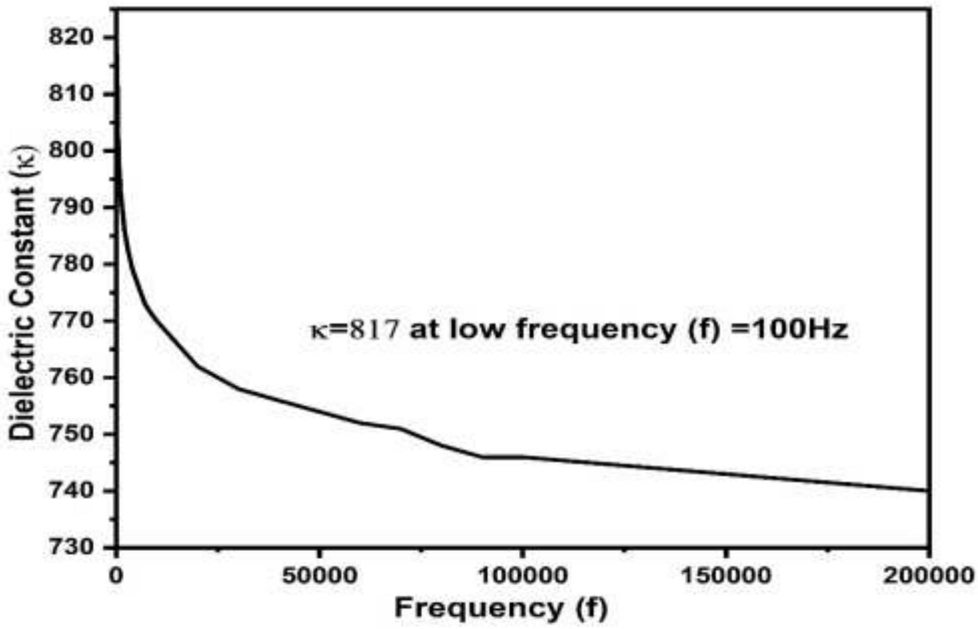

Fig. 6 Graph of Dielectric constant (k) Vs Frequency (Hz)

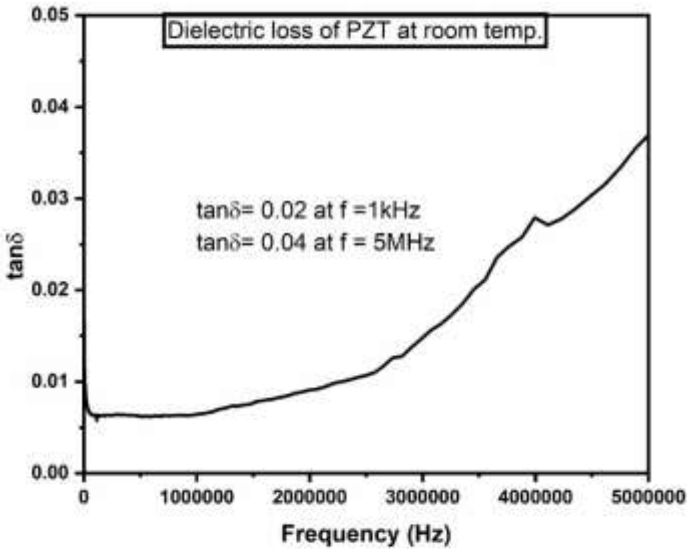

Fig. 7 Dielectric loss (tanδ) Vs Frequency (Hz)

For dielectric properties measurement, Make the PZT pallet by using the hydraulic pressed machine. The powder pressed at high pressure and having the diameter is 0.9cm and thickness is 3mm.The PZT pallet is sintered at 700^0C for 1 hour. After, pallet was painted both side by using silver paste which acts as electrodes. The experimental was carried out from 100Hz to 200 kHz at room temperature. The figure 6 and figure 7 are shows the graph of dielectric constant (k) and dielectric loss with frequency at room temperature. From the figure it is observed that, *k* values decrease gradually with increase in the frequency. The value of dielectric constant (k) at 100 Hz is found 817 and dielectric loss (D) is found 0.02. The large value of k of PZT at lower frequency because, all polarizations (electronic, ionic, orientation and space charge) contribute. The large value of dielectric constant at low frequency arises due to the presence of space charge polarization near the grain boundaries interfaces which depend on the purity and perfection of the sample. When frequency increased, the orientation polarization decreases since it takes more time than electronic and ionic polarization. This decreases value of relative dielectric constant value at higher frequency correspondingly to interfacial polarization.

4.6 Ferroelectric properties:

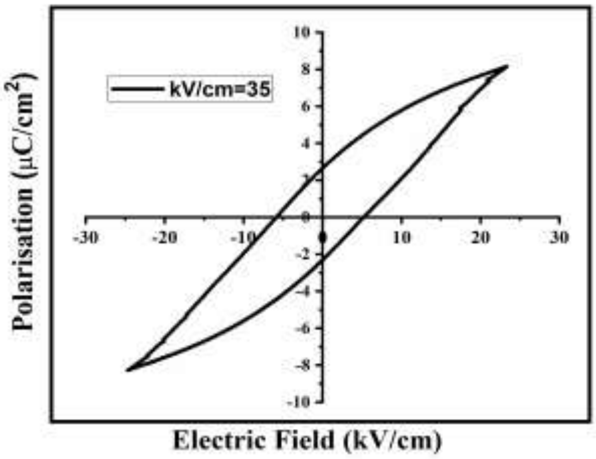

Fig.8 P-E loop of PZT

Figure 8 shows the PE loop of PZT. The measured polarization verses applied electric field curve of PZT pallet sintered at 700^0C polled at 35kV/cm is illustrated in figure. From the figure it is observed that the remnant polarization (P_r) is 2.7 μC/cm^2, the coercive field is 5.1kV/cm and saturation polarization (P_s) is 8kV/cm**.** In PZT, Zr^{4+} and Ti^{4+} are body centered and O^{2-} ions at face centered. When DC potential applied across the PZT pallet. The bond length between Zr^{4+} /Ti^{4+} ions and the O^{2-} (oxygen) ions is changed means these ions change the dipole. In PZT materials behaves like ferroelectric, because all dipoles are aligned to the same direction with respect to the direction of applied electric field. The dipoles are separated by the boundaries are called domain boundaries. In this domain, all neared domains are antiparallel to one another. Therefore, total dipole moment is zero. When Dc potential across the PZT pallet is removed, some dipoles are aligned in the direction of applied potential. This property is called remanent polarization and it is useful for energy storage devices and memories devices.

Conclusion: -

The $PbZr_{0.52}Ti_{0.48}O_3$ (PZT) nanocrystals were effectively produced through a sol–gel synthesis route, and composite films were fabricated by blending these nanoparticles with polycarbonate at multiple concentration levels. The resulting PZT material was examined using XRD, FTIR, UV–Vis, and SEM techniques to evaluate its structure, bonding, optical properties, and surface morphology. Both XRD and FTIR analyses verified the development of a perovskite PZT phase at 700 °C, with no evidence of pyrochlore formation. The diffraction pattern confirms that the particles adopt a tetragonal crystal symmetry, with an estimated crystallite dimension of nearly 26.5 nm. FTIR spectra further highlight characteristic metal–oxygen vibrational features within the 400–800 cm^{-1} region. UV–Vis spectroscopy reveals that the synthesized PZT exhibits a band gap close to 3 eV. SEM images demonstrate that the particles are mainly spherical in appearance and show a tendency toward agglomeration, which is common in sol–gel derived powders. Electrical characterization indicates that the PZT sample possesses a dielectric constant of 817 at 100 Hz, gradually reducing to 740 at higher frequencies, while the dielectric loss remains low at 0.02. Ferroelectric measurements of the pellet sintered at 700 °C show a defined P–E response, with a remanent polarization (Pr) of 2.7 μC/cm², a saturation polarization (Ps) of 8 kV/cm, and a coercive field (Ec) of 5.1 kV/cm.

References:

1. Zr, P., Fe, T. X. O. X., Khorrami, G. H., Zak, A. K., & Banihashemian, S. M. (2014). Magnetic and dielectric properties on sol – gel combustion synthesis. *ADVANCED POWDER TECHNOLOGY*, *3*, 1–6. https://doi.org/10.1016/j.apt.2014.03.011
2. Nano-powders, T. (2006). *Sol – Gel Processing and Characterization of Phase-Pure Lead Zirconate*. *2037*(20874), 2034–2037. https://doi.org/10.1111/j.1551-2916.2006.01002.x
3. Zak, A. K., & Majid, W. H. A. (2011). *Effect of solvent on structure and optical properties of PZT nanoparticles prepared by sol – gel method , in infrared region*. *37*, 753–758. https://doi.org/10.1016/j.ceramint.2010.10.020
4. Yu, H., & Shin, C. (2021). *Impact of Rapid-Thermal-Annealing Temperature on the Polarization Characteristics of a PZT-Based Ferroelectric Capacitor*. 4–9.
5. Desai, K. R., Pathan, A. A., & Bhasin, C. P. (2017). *Synthesis , Characterization of Cadmium Sulphide nanoparticles and its Application as Photocatalytic degradation of Congored*. *43*(2), 39–43.
6. Su, A. (2008). *On the synthesis and crystallization process of nanocrystalline PZT powders obtained by a hybrid sol – gel alkoxides route*. *450*, 380–386. https://doi.org/10.1016/j.jallcom.2006.10.143
7. K. Lu, Sintering of nanoceramics, Int. Mater. Rev. Vol. 53[1] (2008) p.21.
8. X.H. Wang and I. W. Chen, Sintering of Nanoceramics, in Yury Gogotsi (Eds.), Nanomaterials Handbook , CRC Press, Boca Raton, USA, 2006, p.12.
9. R. Chaim, M. Levin, A. Shlayer, et al., Sintering and densification of nanocrystalline ceramic oxide powders: a review, Adv. Appl. Ceram. Vol. 107[3] (2008) p.159-169.
10. Y. Saito, H. Takao, T. Tani, et al., Lead-free piezoceramics, Nature Vol. 432[7013] (2004) p.84-87.
11. J. Frantti, Notes of the Recent Structural Studies on Lead Zirconate Titanate, J. Phys. Chem. B Vol.112[21] (2008) p.6521-6733.
12. A. Suarez-Gomez, R. Sato-Berru, R. A. Toscano, et al.: J. Alloy. Compd. Vol.450[1-2] (2008) p.380.
13. S. Linardos, Q. Zhang, and J. R. Alcock, Preparation Of Sub-Micron PZT Particles With The Sol-Gel Technique, J. Eur. Ceram. Soc. Vol. 26[1-2] (2006) p.117-123.
14. Y. Faheem and M. Shoaib, Sol–Gel Processing and Characterization of Phase-Pure Lead Zirconate Titanate Nano-Powders, J. Am. Ceram. Soc. Vol.89[6] (2006) p.2034-2037.
15. R. M. Piticescu, A. M. Moisin, D. Taloi, V. Badilita, and et al., Hydrothermal synthesis of ultradisperse PZT powders for polar ceramics, J. Eur. Ceram. Soc. Vol.24[6] (2004) p.931-935. 17. A. Y. Wu, P. M. Vilarinho, I. M. M. Salvado, and et al., Sol–Gel Preparation of Lead Zirconate Titanate Powders and Ceramics: Effect of Alkoxide Stabilizers and Lead Precursors, J. Am. Ceram. Soc. Vol.83[6] (2000) p.1379-1385.
16. M. Kakihana, L. Borjesson, S. Eriksson, and et al., Fabrication and characterization of highly pure and homogeneous YBa2Cu3O7 superconductors from sol-gel derived powders, J. App. Phys. Vol.69[2] (1991) p.867-873.
17. Y. K. Sun, Synthesis and Electrochemical Studies of Spinel Li1.03Mn2O4 Cathode Materials Prepared by a Sol-Gel Method for Lithium Secondary Batteries, Solid State Ionics Vol. 100[1-2] (1997) p.115-125.

18. Z. X. Yue, J. Zhou, L. T. Li, et al., Synthesis of nanocrystalline NiCuZn ferrite powders by sol-gel auto-combustion method, J. Magn. Mater., Vol. 208[1-2] (2000) p.55-60.
19. W. Zhao, X.H. Wang, J. Hao, et al., Preparation and Characterization of Nanocrystalline (1-x)BiScO3-xPbTiO3 Powder, J. Am. Ceram. Soc., Vol. 89[4] (2006) p.1200-1204.